

# Dynamics of Line-Driven Disk Winds in Active Galactic Nuclei II: Effects of Disk Radiation

Daniel Proga<sup>1,2</sup> and Timothy R. Kallman<sup>3,4</sup>

## ABSTRACT

We explore consequences of a radiation driven disk wind model for mass outflows from active galactic nuclei (AGN). We performed axisymmetric time-dependent hydrodynamic calculations using the same computational technique as Proga, Stone and Kallman (2000). We test the robustness of radiation launching and acceleration of the wind for relatively unfavorable conditions. In particular, we take into account the central engine radiation as a source of ionizing photons but neglect its contribution to the radiation force. Additionally, we account for the attenuation of the X-ray radiation by computing the X-ray optical depth in the radial direction assuming that only electron scattering contributes to the opacity. Our new simulations confirm the main result from our previous work: the disk atmosphere can 'shield' itself from external X-rays so that the local disk radiation can launch gas off the disk photosphere. We also find that the local disk force suffices to accelerate the disk wind to high velocities in the radial direction. This is true provided the wind does not change significantly the geometry of the disk radiation by continuum scattering and absorption processes; we discuss plausibility of this requirement. Synthetic profiles of a typical resonance ultraviolet line predicted by our models are consistent with observations of broad absorption line (BAL) QSOs.

*Subject headings:* accretion disks – outflows – active galactic nuclei – methods: numerical

---

<sup>1</sup>JILA, University of Colorado, Boulder, CO 80309-0440, USA

<sup>2</sup>proga@colorado.edu

<sup>3</sup>LHEA, GSFC, NASA, Code 662, Greenbelt, MD 20771, USA

<sup>4</sup>tim@xstar.gsfc.nasa.gov

## 1. INTRODUCTION

Radiation pressure on spectral lines (line force) driving a wind from an accretion disk is the most promising hydrodynamical (HD) scenario for AGN outflows. Within this framework, a wind is launched from the disk by the local disk radiation at radii where the disk radiation is mostly in the ultraviolet (UV; e.g., Shlosman, Vitello & Shaviv 1985; Murray et al. 1995, MCGV hereafter). Such a wind is continuous and has mass loss rate and velocity which are capable of explaining the blueshifted absorption lines observed from many AGN, if the ionization state is suitable. Such winds have the desirable feature that they do not rely on unobservable forces or fields for their motive power. However, detailed tests of this idea via modelling is challenging. The wind dynamics are coupled to the ionization and opacity properties of the gas, and the location and nature of the radiation sources is not well understood. Previous models by us (Proga Stone and Kallman 2000, hereafter PSK) relied on UV radiation from the black hole in order to make the flow steady and to impart a strong radial component. In this paper we report new calculations which relax this requirement, and which demonstrate quantitative consistency between disk winds and observations.

UV driven disk winds in AGN are motivated by analogy with winds from hot stars, which have been explored in great detail (eg. Lamers and Cassinelli 1999 and references therein). But they differ in important ways, including the role of rotation near a Keplerian disk, the non-uniform disk temperature distribution, and the influence of the strong X-ray flux from the inner disk and black hole. Rotation acts to make the vertical component of gravity increase with height near the disk plane, and can also affect the wind trajectory when height is comparable to the radius. Close to the disk plane the wind is driven by photons emitted locally, but at greater heights the radiation spectrum and the driving momentum depend on position; the increase in disk temperature at small radius can result in a net outward component to the momentum. The wind density and mass loss rate can be estimated from the observed AGN UV luminosity. When compared with the X-ray flux from the AGN, the density is low enough that the gas is predicted to be highly ionized. If so, the opacity needed for efficient driving and for line formation will be very small and the wind will fail. On the other hand, estimates for the column density in the radial direction close to the disk surface are high enough that a portion of the wind can be shielded from this ionization. Viable models for disk winds must account self-consistently for the wind driving, ionization, and self shielding. MCGV pointed this out and postulated the existence of ‘hitchhiking’ gas which is not driven by UV but which provides the shielding. Their calculation was a one-dimensional time independent quasi-radial flow. Proga, Stone & Kallman (2000, PSK hereafter) were able to relax some of the MCGV assumptions, and explored consequences of a radiation driven disk wind model by performing 2.5 dimensional time-dependent HD simulations. The most challenging component of fluid dynamics calculations is treatment of

the radiative transfer. In the case of disk wind calculations this limitation forces an inexact treatment of the radiative transfer, by assuming parameterized values for the X-ray and UV continuum opacities.

PSK found that a disk accreting onto a  $10^8 M_\odot$  black hole at the rate of  $1.1 \text{ g s}^{-1}$  ( $1.8 M_\odot \text{ yr}^{-1}$ ) can launch a wind at  $r_l \sim 10^{16} \text{ cm}$  from the central engine. The X-rays from the central object are significantly attenuated by the disk atmosphere so they cannot prevent the UV radiation from pushing matter away from the disk. However, the X-rays can overionize the gas in the flow high above the disk and decrease the wind velocity. For a reasonable X-ray opacity, e.g.,  $\kappa_X = 40 \text{ g}^{-1} \text{ cm}^2$ , the disk wind can be accelerated by the central UV radiation to velocities of up to  $15000 \text{ km s}^{-1}$  at a distance of  $\sim 10^{17} \text{ cm}$  from the central engine. The covering factor of the disk wind is  $\sim 0.2$ . The wind is unsteady and consists of an opaque, slow vertical flow near the disk that is bounded on the polar side by a high-velocity stream. A typical column density radially through the fast stream is a few  $10^{23} \text{ cm}^{-2}$  so that the stream is optically thin to the UV radiation but optically thick to the X-rays.

A key issue in modeling radiation pressure driven winds from disks is the relative importance of the driving by photons emanating from near the black hole, i.e. at radii smaller than the computational grid, compared with photons emitted by the disk at radii within the computational grid. Models for CV disk winds, which resemble AGN disk winds except for an absence of strong X-rays, show that strong steady flows require a central source of UV. Motivated by this, PSK as well as MCGV considered the situation where the central radiation in the UV accelerates the gas in the radial direction. A consequence of this assumption is that an efficiently driven wind must attenuate the X-rays, in order to avoid over-ionization, but must transmit the UV, in order to be driven. This places an intrinsic limit on the radial column density, and hence on the mass loss rate, and can also influence the geometry of the flow.

Our goal in the present paper is to explore what happens when the assumption of a strong central flux is relaxed in the PSK models, and to examine other consequences of the line-driven disk wind model. In particular, we check how robust is the disk wind solution and whether the solution predicts synthetic line profiles capable of reproducing line profiles observed in AGN. In §2, we summarize the key elements of our calculations. We present the results from disk wind simulations and synthetic line profile calculations in §2.1 and §2.2, respectively. The paper ends in §4, with our conclusions and discussion.

## 2. METHOD

In this paper we extend work by PSK by relaxing some of their assumptions and simplifications. Our 2.5-dimensional HD numerical method is in most respects as described by PSK. Here we only describe the key elements of the method and list the changes we made. We refer a reader to PSK for details.

As in PSK, we apply line-driven stellar wind models (Castor, Abbott & Klein 1975, hereafter CAK) to winds driven from accretion disks (see also Proga, Stone & Drew 1998; 1999, PSD98 and PSD99 hereafter). We specify the radiation field of the disk by assuming that the temperature follows the radial profile of the optically thick accretion disk (Shakura & Sunyaev 1973). We account for some of the effects of photoionization. In particular, we calculate the gas temperature assuming that the gas is optically thin to its own cooling radiation. We also take into account some of the effects of photoionization on the line force. In particular, we compute the parameters of the line force using a value of the photoionization parameter,  $\xi$  and the analytical formulae due to Stevens & Kallman (1991). This procedure is computationally efficient and gives approximate estimates for the number and opacity distribution of spectral lines for a given  $\xi$  without detail information about the ionization state (see Stevens & Kallman 1991). Additionally, we take into account the attenuation of the X-ray radiation by computing the X-ray optical depth in the radial direction.

We modify PSK’s method as follows: (i) we decrease the inner and outer radius of the computational domain (see §3 for details); (ii) to compute the radiation force due to lines, we use the intensity of the radiation integrated over the UV band only (i.e., between 200 Å and 3200 Å, see also Proga 2003). (in PSK we took the UV flux to be a constant fraction of the flux from the black hole); (iii) we exclude entirely the central object radiation force; (iv) we compute the X-ray optical depth in the radial direction by considering only electron scattering (in PSK we took the X-ray opacity to be  $\kappa_X = 40 \text{ g}^{-1} \text{ cm}^2$ ); (v) we do not explicitly treat continuum opacity for photons emitted from the disk, although the self-shielding of the lines is taken into account by our Sobolev treatment of the line force (in PSK we allowed the disk radiation to be attenuated in the radial direction with an opacity  $\kappa_{UV} = 0.4 \text{ g}^{-1} \text{ cm}^2$ ).

The changes in our calculations extend the range of validity of calculations of PSK. The decrease of the inner radius of the computation domain allows us to capture as much as possible of the UV emitting disk within our grid. The second change makes our calculations as self-consistent as possible without making them computationally prohibitive, i.e., there is no wind launching from very large radii where the disk is cold and radiates few UV photons, and from very small radii where the disk effective temperature or gas temperature, or both, are too high to permit enough spectral lines. The third change was motivated by the results

from PSK: we want to test the importance of attenuation of the central UV flux as a limit to the acceleration of gas to high velocities, and also the extent to which the central flux is needed to make a strong and steady flow. By neglecting the radiation force from the central object we are exploring relatively unfavorable conditions for wind acceleration. The only force that can accelerate the wind is the radiation force due to the disk. The fourth change was also motivated by our wish to explore relatively unfavorable conditions for attenuation of X-rays by disk winds. Using this treatment, our method gives a lower limit for the optical depth to ionizing photons. The fifth change to the calculations means that we allow all disk photons emitted toward a given point in the wind to reach this point. This may correspond to an overestimate of the disk radiation force. However, exact transfer of UV continuum is computationally prohibitive and is treated in the Sobolev approximation even in one dimensional hot star wind models. We briefly discuss some of the consequences of our changes in §.4.

### 3. RESULTS

We present here results for the same model parameters as in PSK with only two exceptions (see below). We assume the mass of the non-rotating black hole,  $M_{BH} = 10^8 M_{\odot}$ . To determine the radiation field from the disk, we assume the mass accretion rate  $\dot{M}_a = 1.8 M_{\odot} \text{ yr}^{-1}$ . These system parameters yield the disk luminosity,  $L_D$  of 50% of the Eddington luminosity and the disk inner radius,  $r_* = 3r_S = 8.8 \times 10^{13} \text{ cm}$ , where  $r_S = 2GM_{BH}/c^2$  is the Schwarzschild radius of a black hole.

The radiation field from the central engine is specified by its luminosity  $L_* = xL_D$  with  $x$  set to 1, its fraction in the UV band ( $f_{UV} = 0.9$ ) and its fraction in the X-rays ( $f_X = 0.1$ ). In PSK,  $f_{UV} = f_X = 0.5$  and these are the only changes to the model parameters we made. The spectral energy distribution of the ionizing radiation is not well known, our choice of values for  $f_{UV}$  and  $f_X$  is guided by the results from Zheng et al. (1997) and Laor et al. (1997) [e.g., see figure 6 in the latter, for a comparison of the spectral energy distributions found for various samples of QSOs.] As mentioned in §2, we include the central radiation only as a source of ionizing photons and exclude its contribution to the radiation force.

There are two definitions of the photoionization parameter used in literature:  $\xi$  and  $U$  (e.g., Krolik 1999). The former is based on the ionizing flux while the latter on the number density of the ionizing photons. For the adopted spectral energy distribution, the conversion between the two is as follows:  $\log U = \log \xi - 1.75$ .

Our computational domain is defined to occupy the radial range  $r_i = 10 r_* \leq r \leq$

$r_o = 500 r_*$ , and the angular range  $0^\circ \leq \theta \leq 90^\circ$ . The  $r - \theta$  domain is discretized into zones. Our numerical resolution consists of 100 and 140 zones in the  $r$  and  $\theta$  directions, respectively. We use fixed zone size ratios,  $dr_{k+1}/dr_k = 1.05$  and  $d\theta_l/d\theta_{l+1} = 1.066$ .

### 3.1. Two component disk wind solution

Figure 1 shows the instantaneous density, temperature and photoionization parameter distributions and the poloidal velocity field of the model. The wind speed at the outer boundary is 2000 to 12000 km s<sup>-1</sup>. This corresponds to a dynamical time of  $\sim 0.2$  yrs for the material at  $\theta \lesssim 60^\circ$ . Figure 1 shows results at the end of the simulation after 6.5 years. Although the flow is still weakly time-dependent after this time has elapsed, the gross properties of the flow (e.g., the mass loss rate and the radial velocity at the outer boundary), settle down to steady time-averages. As in the flow found by PSK, the wind has 3 components: (i) a hot, low density flow in the polar region (ii) a dense, warm and fast equatorial outflow from the disk, (iii) a transitional zone in which the disk outflow is hot and struggles to escape the system. The main difference with the results of PSK is that here the transitional zone is much more prominent, and it occupies a large fraction of the computational domain.

In the polar region, the density is very small and close to the lower limit that we set on the grid, i.e.,  $\rho_{min} = 10^{-20}$  g cm<sup>-3</sup>. The line force is negligible because the matter is highly ionized as indicated by a very large photoionization parameter ( $\sim 10^8$ ). The gas temperature is close to the Compton temperature of the X-ray radiation. The matter in the polar region is pulled by the gravity from the outer boundary, which is an artifact of the boundary conditions (e.g., we do not model a jet which is likely to propagate through the polar region). However, this region is sometimes filled with gas which is launched from the disk with a large vertical velocity in an episodic manner.

The outflowing wind itself has distinct two components: hot and warm. The two components are launched from the disk by the line force. The gas density at the disk atmosphere and wind base is  $\sim 10^{-12}$  g cm<sup>-3</sup>, so the photoionization parameter is low ( $\log(\xi) \leq -5$ ) despite the strong central radiation. However as the flow from the inner part of the disk is accelerated by the line force its density decreases. For the disk wind launched at small radii ( $r \gtrsim r_i$ ), this decrease of the density causes an increase in the gas temperature and the photoionization parameter. As this process proceeds the gas becomes fully ionized and loses all driving lines. The wind speed when this happens is not generally great enough to allow the gas to escape, and it tends to fall back toward the disk. This ‘failed wind’ has an effect on the remainder of the flow, both due to its shielding effect on the central X-rays and due

to its pressure as it falls toward the disk.

The disk wind launched at large radii does not become overionized downstream despite a density decrease. The photoionization parameter in this wind is kept low because of the large column density toward the source of the ionizing photons. Consequently, the outer disk wind is not only launched but also accelerated by the disk line force. We find that the outer wind becomes radial relatively close to the disk. This may seem surprising because we set to zero the radiation force in the radial direction due to the central object. There are three effects responsible for the flow to be equatorial: (i) overionization of the vertical part of the wind by the central object radiation; (ii) the ram pressure of the failed wind launched at smaller radii that falls back after it is overionized; and (iii) the line force due to disk photons emitted interior to a given point in the wind. The two first effects dominate at smaller radii and close to the interface between the hot and warm flow whereas the third effect dominates above the disk at large radii where the fore-shortening of the disk radiation weakens.

The flows we find are time dependent and have density and velocity fluctuations of  $\sim 10^2$  even after the flow has evolved for many dynamical times. In particular, there are occasionally regions along the equator with the gas densities lower than those for hydrostatic equilibrium. From those low density regions, the radiation force can launch a wind with an acceleration length scale shorter than for a CAK-like wind [the line force is a strong function of the gas density (CAK)]. In fact, we observe that the line acceleration can be so efficient that some gas can reach velocities comparable to the escape velocity before it is eventually overionized. This flow behavior manifests itself as erratic high velocity ejections of gas from the inner disk.

Figure 2 presents the run of the density, radial velocity, mass flux density, accumulated mass loss rate, photoionization parameter and column density as a function of the polar angle,  $\theta$ , at the outer boundary,  $r = r_o = 4.422 \times 10^{16}$  cm from Figure 1. The accumulated mass loss rate,  $\dot{m}$  and the column density,  $N_H$  are computed as in PSK (see eq. 13 in PSD 98 and eq. 24 in PSK for the definitions of  $\dot{m}$  and  $N_H$ , respectively). The gas density is very low, i.e.,  $\rho_{min} = 10^{-20}$  g cm $^{-3}$ , for  $\theta$  between  $0^\circ$  and  $5^\circ$ . Then the gas density increases with  $\theta$  between  $5^\circ$  and  $45^\circ$  to the level of a few  $\times 10^{-18}$  g cm $^{-3}$ . For  $45^\circ \lesssim \theta \lesssim 55^\circ$ , the density decreases to the level of  $\rho_{min} = 10^{-20}$  g cm $^{-3}$  at  $\theta = 55^\circ$ . Then the density increases again with  $\theta$  and reaches the maximum of a few  $\times 10^{-18}$  g cm $^{-3}$  at  $\theta = 75^\circ$ . This is followed by a decrease of the density with the minimum of a few  $\times 10^{-20}$  g cm $^{-3}$  at  $\theta = 88^\circ$ . For,  $\theta > 88^\circ$ , the density sharply increases, as might be expected of a density profile determined by hydrostatic equilibrium. The radial velocity is  $-2000$  km s $^{-1}$  for  $0^\circ \lesssim \theta \lesssim 5^\circ$  and has a broad flat maximum at the level of  $3000$  km s $^{-1}$  for  $\theta$  between  $5^\circ$  and  $55^\circ$ . For  $\theta$  between  $55^\circ$  and  $60^\circ$ , the radial velocity is negative and then gradually increases to  $20000$  km s $^{-1}$  at

$\theta \lesssim 85^\circ$ . This is followed by a drop of  $v_r$  to a very small value near the equator. We note that  $v_r$  stays nearly constant at the level of  $12000 \text{ km s}^{-1}$  for  $72^\circ \lesssim \theta \lesssim 82^\circ$ .

The accumulated mass loss rate is negligible for  $\theta \lesssim 35^\circ$  because of the very low gas density and velocity. For  $\theta \gtrsim 35^\circ$ ,  $\dot{m}$  increases to  $\sim 1 \times 5 \times 10^{23} \text{ g s}^{-1}$  at  $\theta \approx 45^\circ$ . For  $\theta$  between  $45^\circ$  and  $67^\circ$ , the accumulated mass loss rate stays nearly constant. For  $\theta \gtrsim 77^\circ$ , the accumulated mass loss rate increases to  $\sim 1.4 \times 10^{25} \text{ g s}^{-1}$  at  $\theta \approx 85^\circ$ .

The column density in the wind increases gradually with  $\theta$ . In particular, it increases from  $\sim 10^{20} \text{ cm}^{-2}$  at  $\theta = 18^\circ$  to  $10^{24} \text{ cm}^{-2}$  at  $\theta = 60^\circ$ . For  $\theta > 60^\circ$ ,  $N_H$  continues to increase and indicates that the wind is optically thick to electron scattering at  $r_o$  for the central object radiation. The column densities greater than  $10^{25} \text{ cm}^{-2}$  are effectively infinite, and represent complete obscuration of the central object. Winds with such high  $N_H$  can still be radiation driven owing to the difference between the column the disk radiation sees and the column the central source radiation sees. We expect that the disk wind obscuration can change the ratio between the number of all QSOs and BAL QSOs, i.e., QSOs, viewed by an observer almost edge-on, would not be detected or identified as QSO.

The photoionization parameter is very high,  $\sim 10^8$ , for  $\theta \lesssim 60^\circ$  because of the very low density in the polar region. However, over next  $7^\circ$ ,  $\xi$  drops by many order of magnitude owing to the increase of the column density. The  $\theta$  profiles of the flow properties show that the overionized outflow can contribute to the total mass loss rate at the level of a few per cent.

Our new simulations of AGN disk wind confirm the main result from PSK: the disk atmosphere can 'shield' itself so that the local disk radiation can launch gas off the disk photosphere. Here we find that this results holds even when the condition for shielding are unfavorable: the ionizing photons are only scattered on electrons but not absorbed by the shielding gas. Our new simulations also provide some new insights to the acceleration. In particular, we find the local disk force suffices to accelerate the disk wind to high velocities in the radial direction provided the wind does not change the geometry of the disk radiation by continuum scattering and absorption processes.

The main difference between our disk wind solution and the solution presented in PSK is the properties and behavior of the hot component of the disk outflow which struggles to escape the system. In PSK, this component occupied a relatively narrow  $\theta$  range ( $\Delta\theta \approx 5^\circ$ ) above the disk wind, whereas here  $\Delta\theta \approx 40^\circ$ . The key reason for this difference is the strength of the radial line force relative to the latitudinal line force acting on the inner disk wind. In PSK, the radial force is strong and accelerates the inner wind on a relatively long length scale (of order of the wind launch radius). A small fraction of the inner flow is overionized and



fails to develop into a strong outflow. This overionized gas falls on the freshly launched disk wind and introduces weak perturbations to the disk wind so that the wind is not significantly slowed down nor disrupted. Here, on the other hand, the radial force is relatively weak and the flow from the innermost disk tends to be vertical. The flow geometry is important for how long the flow can stay shielded: for the vertical geometry, the flow height can be larger than the height of the shielding gas whereas for the radial geometry, the flow height can stay smaller than the height of the shielding gas even at very large distances from the launch point. Therefore vertical flow is more susceptible to overionization than radial flow; a much larger fraction of the inner flow is overionized in the vertical flow than in the radial flow. In our simulations the overionized flow is relatively dense and as it falls on the disk it disrupts the freshly launched the disk wind.

We note that the mass loss rate in our simulations is smaller than in PSK’s simulation by a factor of  $\sim 2$ . This is an unexpected result because here we allow launching a wind from radii smaller than those in PSK and a simple scaling law for line-driven disk wind models suggests that mass loss rate should increase with decreasing radius (e.g., PSD98; Proga & Kallman 2002). Additionally, one can argue that because of this scaling, overionization should become less of a problem with decreasing radius (Proga & Kallman 2002). What is then responsible for this low mass loss rate? Our analysis of the flow properties and time evolution shows that at the early phase of the evolution, the mass flux density is consistent with the expectations based on the above arguments. However, as the inner disk wind becomes overionized and starts falling back toward the equator the mass loss rate decreases because the average gas density at the wind base increases which reduces the driving line force. Additionally, the infalling gas is dense and can significantly slow the outflow which it encounters on its way toward the disk. There are then a few factors which reduce the mass loss rate but the primary factor is the flow overionization.

Our time-dependent disk wind solutions differ from those found by PSD98, in which it was shown that CV disk winds are unsteady in time when the wind is driven solely by disk radiation. In the latter, the flow could also fall back on the disk, but it was not strong enough to cause a significant decrease in the mass loss rate. Furthermore, in the PSD98 simulations there was no radiation capable of fully ionizing the wind so that regions of relatively low density, above the falling gas, could be accelerated to high velocities and contribute to the total mass loss rate.

### 3.2. UV absorption line profiles

Simulations presented in PSK and here can serve as a proof-of-concept for the radiation driven disk wind model of outflows in AGN. Some consequences of the radiation driven disk wind model have been explored in the context of CV and low mass X-ray binaries (LMXB; e.g., see PSD98 and Proga & Kallman 2002, respectively). Generally, the insights from those models allow us to explain systems with strong evidence for UV absorbing disk wind – such as CVs – and systems without UV absorbing disk wind – such as LMXB. In the case of CVs, the model also predicts UV line profiles which are capable of reproducing observations (Proga 2003). In this section, we present synthetic line profiles predict by our model and briefly discuss their relevance to AGN observations.

We present line profiles for the C IV  $\lambda 1549$  transition. We compute the profiles by integrating flux from the entire disk at a given orientation (i.e., as in the dynamical models, the continuum source has a finite size). The line profile calculation performed here are exactly as in Proga et al. (2002) with the exception that we set the C IV abundance to one in the regions with the gas temperature from 8000 K to 420000 K and to zero elsewhere. For the adopted model parameters, the upper limit for the gas density corresponds to the disk effective temperature at  $r_i$ . We refer a reader to Proga et al. (2002) for details on line-profile calculations.

The C IV abundance could be in principle, computed self-consistently for given wind structure and radiation field. However, we save this for a future paper and focus on gaining some insights from the multidimensional models of disk winds and predicted profiles.

To illustrate the effect of viewing angle on the line profiles, Figure 3 shows line profiles for five inclination angles:  $i = 60^\circ, 65^\circ, 70^\circ, 75^\circ$ , and  $80^\circ$ . We limit our line profile calculation to the absorption contribution only. Modeling of the emission component depends on the influence of thermal line emission, and we will discuss this in a future paper. Figure 3 clearly shows that the line profiles are very sensitive to the inclination angle. In particular, for  $i = 65^\circ$  the line absorption is broad and nearly symmetric whereas for  $i$  just  $5^\circ$  higher a strong blueshifted absorption dominates the line profile (compare figs 3c and 3d). We note that for  $i = 60^\circ$  the profiles is more symmetric than for  $i = 65^\circ$ . In the latter case, the blueshifted absorption is somewhat stronger than the redshifted absorption. Overall our line profiles are representative of generic line profiles for a bipolar wind from a rotating disk (e.g. Proga et al. 2002 and references therein). For example, for a relatively high inclination angles ( $i \gtrsim 50^\circ$ ) the profiles are affected by the absorption in the rotating base of the wind, so blueshifted as well as redshifted absorption is present (see Proga et al. 2002, and references therein). The presence of the expanding wind manifests itself in the profiles by a blueshifted absorption for inclination angles where the continuum source is viewed

through the expanding wind. In our wind model, the disk wind with a low  $\xi$  (i.e., high C IV abundance) has a half-opening angle of  $\sim 65^\circ$ . Therefore only for  $i \gtrsim 60^\circ$ , our line profiles show blueshifted absorption stronger than redshifted absorption.

In general, the line profiles predicted by our models are similar to those predicted by the model for CV winds (Proga 2003). However, there are two important differences: (i) for low  $i$ , CV wind models predict a blueshifted absorption whereas here little absorption is present at those angles and (ii) for all  $i$ , CV wind models predict that the maximum of the blueshifted absorption is line-centered whereas here the maximum can be blueshifted by as much as  $5000 \text{ km s}^{-1}$ . The reason for these differences is the fact that in CV wind models, the base of the wind covers the whole continuum source whereas here the continuum source extends inside the computational domain and therefore the continuum is only partially covered by the flow.

Our line profiles are consistent with many of the properties of profiles observed in broad absorption line QSOs (e.g., Korista et al. 1993; Hall et al 2002). In particular, the synthetic line profiles can be as strong and broad (up to  $30000 \text{ km s}^{-1}$ ) as those observed. Additionally, for certain inclination angles the maximum of the blueshifted absorption is far from the line center - this is consistent with so-called detached troughs observed in some QSOs. Some of the profiles shown in Fig. 3 display prominent redshifted absorption. In observed lines, this component is likely to be affected by the emission contribution to the line (e.g., Proga 2003). The line emission can fill in the redshifted absorption and also some of the highly blueshifted absorption produced by the wind near the equator where the rotational velocity exceeds the expansion velocity. For example, Proga (2003) showed that for high inclinations ( $i > 80^\circ$ ), the profile has double-peaked emission (figs. 1e and 1j in Proga 2003).

#### 4. CONCLUSIONS AND DISCUSSION

In this paper we have presented numerical simulations of the radiation-driven disk wind scenario for AGN outflows. These models provide insights into the wind’s capability to shield itself from ionizing radiation. We performed axisymmetric time-dependent hydrodynamic calculations similar to those of Proga, Stone and Kallman (2000). We studied the robustness of the radiation launching and acceleration of the wind for relatively unfavorable conditions. In particular, we have taken into account the central engine radiation as a source of ionizing photons but neglected its contribution to the radiation force. Additionally, we have accounted for the attenuation of the X-ray radiation by computing the X-ray optical depth in the radial direction assuming that only electron scattering contributes to the opacity. Our new simulations confirm the main result from PSK: the disk atmosphere can ‘shield’ itself

from external X-rays so that the local disk radiation can launch gas off the disk photosphere. We have also found that the local disk force suffices to accelerate the disk wind to high velocities in the radial direction. This is true provided the wind does not change significantly the geometry of the disk radiation by continuum scattering and absorption processes, and we discuss the plausibility of this requirement. Overall our models are consistent with observations of broad absorption line (BAL) QSOs. Additionally, synthetic profiles of a typical resonance ultraviolet (UV) line, predicted by our models, promise to reproduce observed BALs and it is likely that the model can account for other AGN outflows observed in UV as well as in X-rays.

Strong ionizing radiation has long been recognized as a serious challenge to theories of AGN outflows absorbing the UV radiation. Radiation-driven disk wind models are particularly affected by this problem because the overionization of the wind can prevent the wind from being driven. But in other models, including a magnetic one, overionization also needs to be addressed owing to the requirement for sufficient un-ionized gas to account for the observed lines. Here we find that an indirect effect of overionization can reduce but not prevent the development of a wind, for our choice of model parameters: the so-called failed inner disk wind. If the density of the failed wind is relatively high then the ram pressure of such a wind can seriously slow down the disk wind which otherwise could be driven by radiation. We emphasize that this damaging effect of the failed wind can be important to explain AGN winds within the radiation driven disk wind scenario rather than being used as an argument against the scenario. In particular, in this scenario the accretion disk, with parameters as adopted here (see §3), should produce a powerful wind from radii as small as  $10^{14} - 10^{15}$  cm because the radiation at those radii is mostly in the UV. However, such a wind would be too fast to be consistent with AGN observations. One of plausible solutions of this problem is to allow for the energy dissipation at small radii to occur not only inside but also outside the disk (i.e., in the disk corona). Consequently, the UV radiation from the innermost disk would be reduced while ionizing radiation would be increased. The two factors would reduce launching of the wind. A complimentary solution is that the failed wind can disrupt development of a wind up to a radius of a few  $\times 10^{15}$  cm.

We have performed many simulations to study the sensitivity of disk wind solutions to the black hole mass and disk luminosity. These results will appear in Proga et al.(2004) (in preparation). Here we only mention that the wind solution is very sensitive to the luminosity compared to the Eddington limit. In particular, we find that for the model parameters as in §.3 but with the luminosity reduced by a factor of 5 (from 50% to 10% of the Eddington limit) there is no disk wind. The primary reason for this luminosity sensitivity is the fact that the mass flux density of the wind decreases strongly with decreasing disk luminosity and the wind is more subject to overionization (e.g. Proga & Kallman 2002). Our simulations

show also that for a fixed Eddington fraction (e.g., 50%) it is easier to produce a wind for  $M_{\text{BH}} \gtrsim 10^7 M_{\odot}$  than for  $M_{\text{BH}} \lesssim 10^7 M_{\odot}$ . This result is a consequence of the decrease of the UV contribution to the disk total radiation with decreasing mass of the BH in the Shakura Sunyaev disk model for a fixed Eddington fraction.

We have also performed many simulations to study the sensitivity of our main results to the model parameters. The most important parameter of the model is the X-ray opacity. This quantity could be computed from first principles for given spectral energy distribution, strength and geometry of the radiation, and the structure and chemical composition of the flow. However, such an approach to  $\kappa_X$ 's calculations is not computationally feasible and therefore we have explored asymptotic approximations, e.g., assuming that  $\kappa_X = 0.4 \text{ g}^{-1} \text{ cm}^2$  (corresponding to the Thomson cross section). As we discussed above, such a simplistic approach yields rather conservative results for the wind strength. In our sensitivity studies, we have computed wind models using a more realistic  $\kappa_X$ . In particular, we computed  $\kappa_x$  based on the analytic fit to the detailed photoionization calculations using the photoionization code XSTAR. We find that  $\kappa_x$  can be expressed a function of the photoionization parameter,  $\xi$  in the following way:  $\kappa_x = \min(10^3, 4 \times 10^3 \xi^{-1.2} + 1)$ , in units of  $0.4 \text{ g}^{-1} \text{ cm}^2$ . We found that as expected a wind with this higher  $\kappa_x$  is stronger (e.g., in terms of  $\dot{M}$  and the opening angle) the model solution described here.

The radiative transfer of continuum photons inside the disk wind is as critical as the wind photoionization structure in modeling disk winds. To accelerate the wind to velocities comparable to the escape velocity we should not rely on the radiation which originates interior to the wind zone because the wind will shield itself from this radiation in the same way as it shields itself from the external ionizing radiation. Here we explore a configuration where the ionizing radiation comes from a point source located at the center while the driving radiation comes from the extended source, (i.e., the UV emitting disk). Calculations of the radiative transfer of the former is relatively simple as it can be approximated by 1D solutions for the optical depth. However, the radiative transfer of the latter is intrinsically 3D and computationally expensive. We argue that the UV continuum photons emitted from the disk into the overlying disk wind can propagate through the disk without large changes of the net radiation flux, hence our assumption that the wind is optically thin to the disk photons. On the other hand, X-rays which are emitted outside the disk wind suffer many scatterings and absorptions once they reach the wind zone. Consequently, the X-rays do not penetrate deep inside the wind zone. The X-ray transfer in the case we consider is analogous to the problem of disk irradiation by an external source whereas the UV transfer is analogous to the problem of radiation transfer in an extended atmosphere.

Our simulations show how the line force can produce a fast, highly ionized wind: if

the density near the wind base is relatively low and the base is shielded over long enough length scale above the disk then the local disk radiation can accelerate gas to relatively high velocities (even exceeding the escape velocity) before the gas becomes overionized. At large radii, such a wind would be transparent to the UV radiation but may be able to absorb X-rays. We plan to present models for the X-ray properties of disk winds in a future paper.

We thank N. Arav, M.C., Begelman, J.R. Gabel, P.B. Hall, G.T. Richards, and J.M. Stone for useful discussions. We also thank an anonymous referee for comments that helped us clarify our presentation. We acknowledge support provided by NASA through grant HST-AR-09947 from the Space Telescope Science Institute, which is operated by the Association of Universities for Research in Astronomy, Inc., under NASA contract NAS5-26555. DP also acknowledges support from NASA LTSA grants NAG5-11736 and NAG5-12867. We acknowledge support from the W. M. Keck Foundation, which purchased the JILA 74-processor Keck Cluster.

## REFERENCES

- Castor, J.I., Abbott, D.C., Klein, R.I. 1975, *ApJ*, 195, 157 (CAK)
- Hall, Patrick B. et al. 2002, *ApJS*, 141, 267
- Korista, K.T., Voit, G. M., Morris, S.L., Weymann, R.J. 1993, *ApJS*, 88, 357
- Krolik, J.H. 1999, *Active galactic nuclei: from the central black hole to the galactic environment*, Princeton, N.J.: Princeton University Press
- Lamers, H.G.J.L.M., and Cassinelli, J., 1999, “Introduction to stellar winds”, Cambridge ; New York : Cambridge University Press.
- Laor, A., Fiore, F., Elvis, E., & Wilkes B.J., & McDowell J.C. 1997, *ApJ*, 477, 93
- Murray, N., Chiang, J., Grossman, S.A., & Voit, G.M. 1995, *ApJ*, 451, 498 (MCGV)
- Proga, D. 2003, *ApJ*, 592, L9
- Proga, D., & Kallman, T.R. 2002, *ApJ*, 565, 455
- Proga, D., Kallman, T.R., Drew, J.E., & Hartley, L.E., 2002, *ApJ*, 572, 382 (Paper 1)
- Proga, D., Stone J.M., & Drew J.E. 1998, *MNRAS*, 295, 595 (PSD 98)
- Proga, D., Stone J.M., & Drew J.E. 1999, *MNRAS*, 310, 476 (PSD 99)

Proga, D., Stone, J.M., & Kallman, T.R. 2000, ApJ, 543, 686 (PSK)

Shakura N.I., & Sunyaev R.A. 1973 A&A, 24, 337

Shlosman, I, Vitello, P.A. & Shaviv G. 1985, ApJ, 294, 96

Zheng, W., Kriss, G.A., Telfer, R.C., Grimes, J.P., & Davidsen, A.F. 1997, ApJ, 475, 469

---

This preprint was prepared with the AAS L<sup>A</sup>T<sub>E</sub>X macros v5.2.

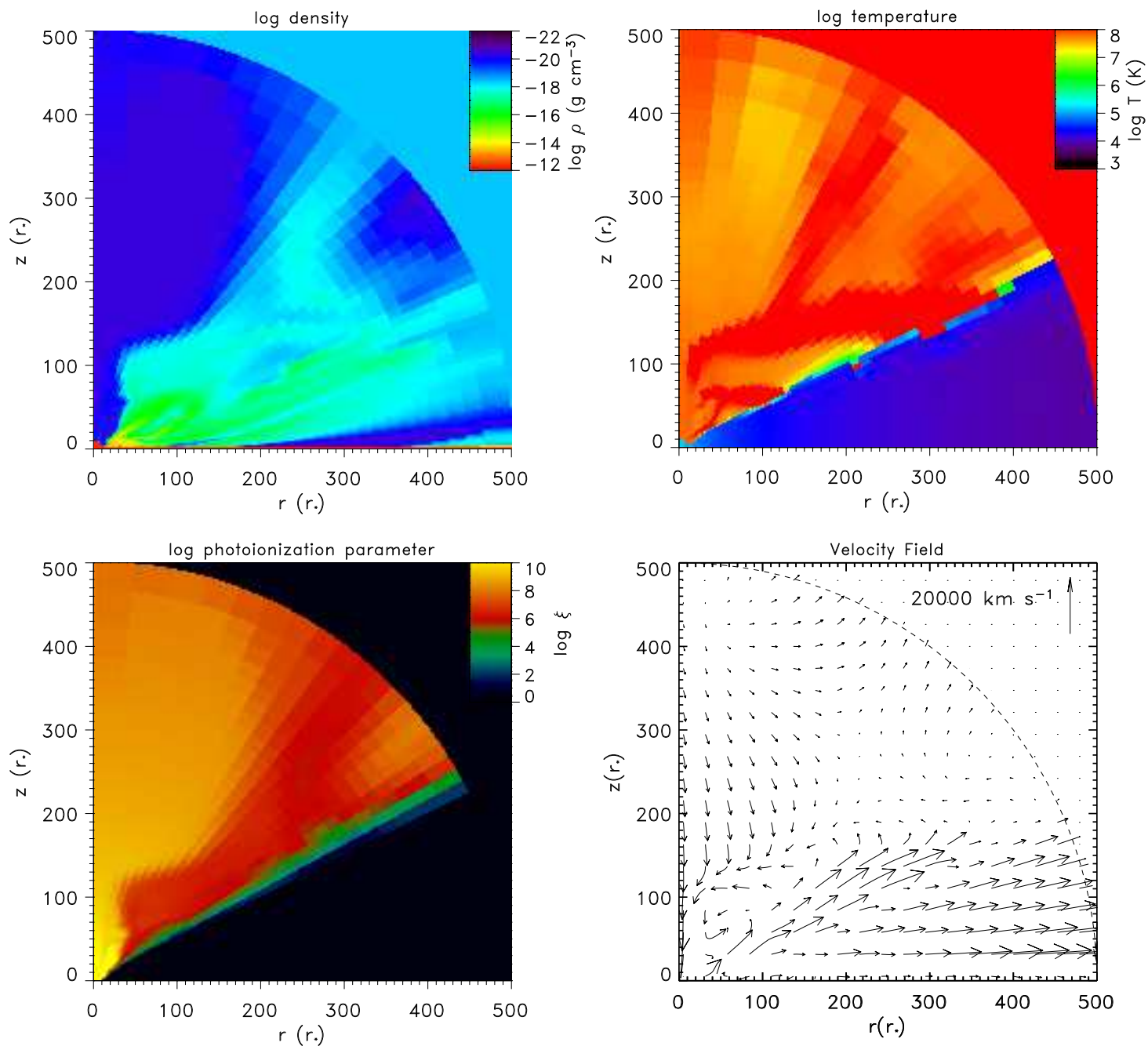


Fig. 1.— The top left panel is a color density map of the AGN disk wind model, described in the text. The top right panel is a color gas temperature map of the model while the bottom left panel is a color photoionization parameter map. Finally, the bottom right panel is a map of the velocity field (the poloidal component only). In all panels the rotation axis of the disk is along the left hand vertical frame, while the midplane of the disk is along the lower horizontal frame.



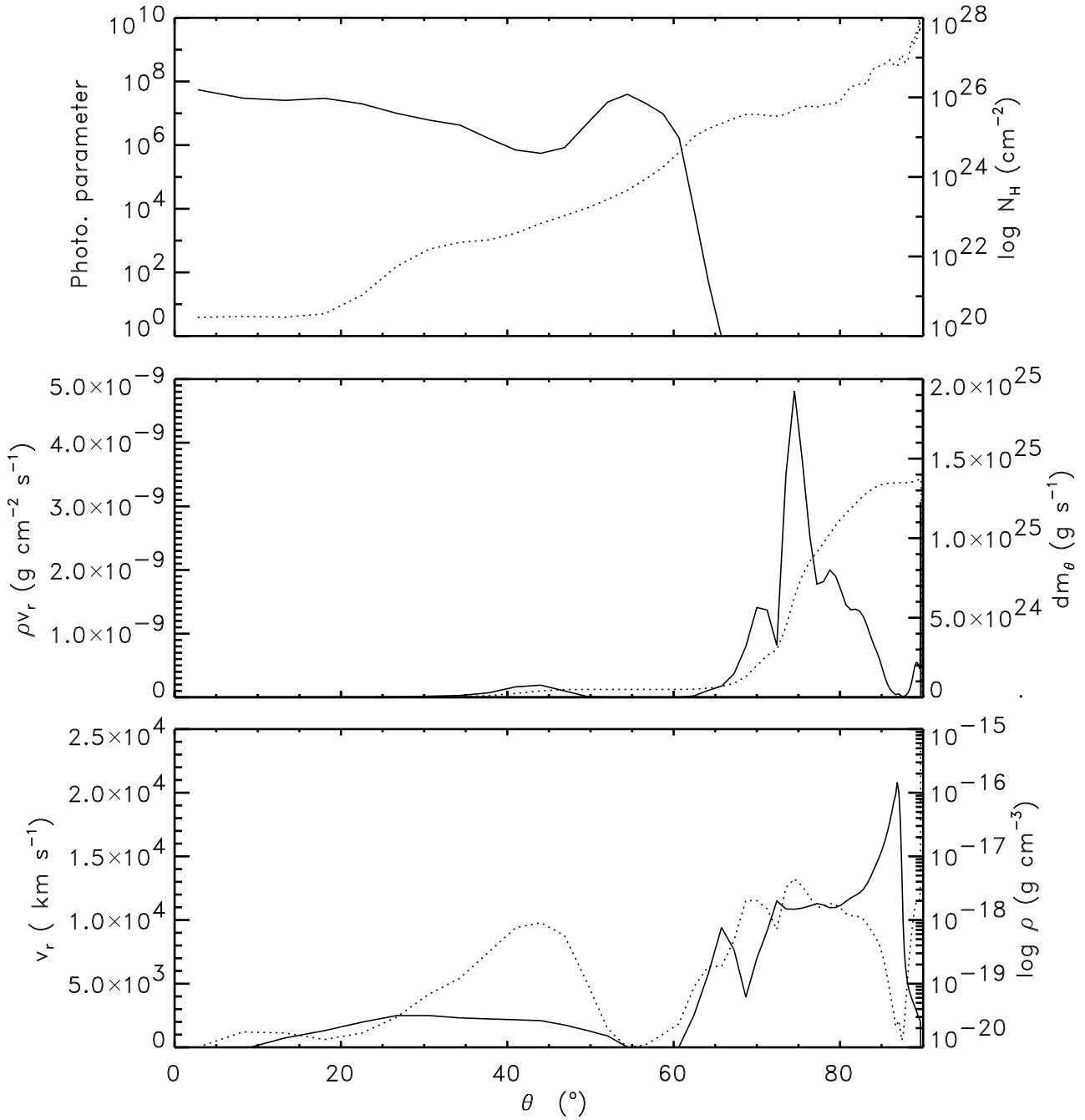


Fig. 2.— Quantities at the outer boundary in our model. The ordinate on the left hand side of each panel refers to the solid line, while the ordinate on the right hand side refers to the dotted line. The column density,  $N_H$  is calculated along the radial direction.

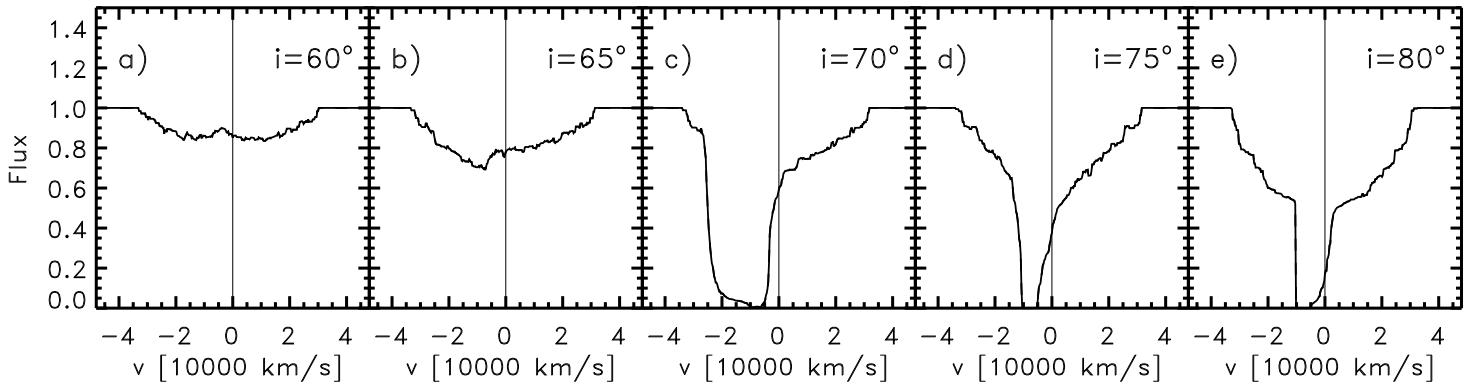


Fig. 3.— Profiles of a resonance ultraviolet line for our hydrodynamical disk wind models as a function of inclination angle,  $i$  (see top right corner of each panel for the value of  $i$ ). The zero velocity corresponding to the line center is indicated by the vertical line.